

# Synthesis, characterization, and electrochemical performance of $\text{LiFePO}_4/\text{C}$ cathode materials for lithium ion batteries using various carbon sources: best results by using polystyrene nano-spheres

Shixi Yu · Shao Dan · Guoen Luo · Wei Liu · Ying Luo · Xiaoyuan Yu · Yueping Fang

Received: 20 March 2011 / Revised: 8 October 2011 / Accepted: 11 October 2011 / Published online: 12 November 2011  
© Springer-Verlag 2011

**Abstract** Olivine  $\text{LiFePO}_4/\text{C}$  cathode materials for lithium ion batteries were synthesized using monodisperse polystyrene (PS) nano-spheres and other carbon sources. The structure, morphology, and electrochemical performance of  $\text{LiFePO}_4/\text{C}$  were investigated by X-ray diffraction (XRD), scanning electron microscopy (SEM), galvanostatic charge–discharge tests, electrochemical impedance spectroscopy (EIS) measurements, and Raman spectroscopy measurements. The results demonstrated that  $\text{LiFePO}_4/\text{C}$  materials have an ordered olivine-type structure with small particle sizes. Electrochemical analyses showed that the  $\text{LiFePO}_4/\text{C}$  cathode material synthesized from 7 wt.% PS nano-spheres delivers an initial discharge capacity of 167  $\text{mAh g}^{-1}$  (very close to the theoretical capacity of 170  $\text{mAh g}^{-1}$ ) at 0.1 C rate cycled between 2.5 and 4.1 V with excellent capacity retention after 50 cycles. According to Raman spectroscopy and EIS analysis, this composite had a lower  $I_D/I_G$ ,  $sp^3/sp^2$  peak ratio, charge transfer resistance, and a higher exchange current density, indicating an improved electrochemical performance, due to the in-

creased proportion of graphite-like carbon formed during pyrolysis of PS nano-spheres, containing functionalized aromatic groups.

**Keywords** Carbon source ·  $\text{LiFePO}_4$  · PS nano-sphere · Lithium ion battery · Cathode material

## Introduction

Lithium ion batteries (LIBs) are the most advanced electrochemical energy storage and conversion systems for a wide range of green applications, including hybrid electric vehicles (HEVs), plug-in hybrid electric vehicles (PHEVs), and stationary energy storage for solar and wind electricity generation, as well as smart grids. However, the current generation of LIBs, using  $\text{LiCoO}_2$  as the cathode material, cannot meet the stringent requirements for high-power applications in terms of cost, safety, and environmental concerns [1, 2]. Lithium iron phosphate ( $\text{LiFePO}_4$ ), with its olivine structure, was first studied by Padhi et al. [3] and has attracted extensive interest as a potential cathode material, particularly for high-power applications, owing to its high theoretical capacity (170  $\text{mAh g}^{-1}$ ), cycling stability, high thermal stability, low cost, and environmental impact. One of the challenging issues in using  $\text{LiFePO}_4$  for high-power LIBs is its low electrical conductivity and low rate capability [4]. Great efforts have been made to improve the electrochemical performance of  $\text{LiFePO}_4$  including: (i) addition of conductive Cu/Ag nanopowders or carbon black powders [5, 6], (ii) doping with supervalent cations [7–10],

S. Yu · S. Dan · G. Luo · W. Liu · Y. Luo · X. Yu (✉) · Y. Fang  
Institute of Biomaterial, College of Science,  
South China Agricultural University,  
Guangzhou 510642, China  
e-mail: yuxiaoyuan@scau.edu.cn

X. Yu  
Key Laboratory of Renewable Energy and Gas Hydrate,  
Chinese Academy of Sciences,  
Guangzhou 510640, China

(iii) coating with carbon layer, metal oxides, and conducting polymers [11–13], and (iv) decreasing the particle size [14, 15].

Recently, efforts to improve the rate capability of  $\text{LiFePO}_4$  have focused on the incorporation of conductive carbon into active material powders, to form carbon-coated  $\text{LiFePO}_4$  ( $\text{LiFePO}_4/\text{C}$ ) composites [16, 17]. Konarova and Taniguchi [18] reported that  $\text{LiFePO}_4/\text{C}$  formed by spray pyrolysis with a wet ball-milling method achieved a high capacity of  $165 \text{ mAh g}^{-1}$  at  $0.1 \text{ }^\circ\text{C}$  rate and an ultrahigh rate capacity of  $130 \text{ mAh g}^{-1}$  at  $5 \text{ C}$  with an excellent cycle life. Chen and Dahn [19] prepared  $\text{LiFePO}_4$  samples containing 3.5 wt.% coated carbon with a discharge of  $160 \text{ mAh g}^{-1}$ . Nakano et al. [20] reported that a  $\text{LiFePO}_4/\text{C}$  composite showed an initial discharge capacity of  $167 \text{ mAh g}^{-1}$  at  $0.1 \text{ C}$  and  $104 \text{ mAh g}^{-1}$  at  $10 \text{ C}$ . In the above literature, modifying  $\text{LiFePO}_4$  particles by coating electronically conductive agent carbon is considered as the effective way to overcome the electronic transport limitations. Obviously, carbon can control particle growth and enhance electronic conductivity, therefore higher capacity and better rate capability can be obtained. Advantages of coated carbon for electrode materials were also suggested by Cushing and Goodenough [21], who proposed that coated carbon improved the electronic conductivity between particles and also provided electronic tunnel to complement the charge equilibrium during Li extraction/insertion.

The properties of  $\text{LiFePO}_4/\text{C}$  composites depend on the phase purity of the active material, particle size, structure of the carbon additive, the carbon content, the form of carbon contact, and the mixing and sintering recipe [4, 22]. It has been reported that the selection of the carbon source, or polymer precursor, is important for tailoring the final properties of carbon-coated composite powders. Recently, it was found that more highly graphitized carbons are formed during pyrolysis when functionalized aromatic or ring-forming compounds are used [23, 24]. Therefore, in this study, we investigated the effects of PS nano-spheres and bamboo fiber as novel two carbon sources on the electrochemical properties of  $\text{LiFePO}_4/\text{C}$  composites, compared with starch, and glucose. In addition, the physical, structural, and electrochemical properties of the  $\text{LiFePO}_4/\text{C}$  composites were systematically investigated.

## Experimental

### Synthesis of mono-disperse PS nano-spheres

Mono-disperse polystyrene (PS) nano-spheres were synthesized as follows: 44 g of styrene (A.R.) was

washed four times with 100 ml of  $0.1 \text{ M NaOH}$  (A.R.), then four times with 200 ml of water. A three-necked, 500 ml round-bottomed flask containing the washed styrene, 0.36 g sodium dodecyl sulfate (A.R.), and 400 ml of water was heated to  $70 \text{ }^\circ\text{C}$  with magnetic stirring. A thermometer, condenser, and pipet, through which nitrogen was bubbled to deaerate the mixture, were attached to the flask. In a separate beaker, 0.45 g of potassium persulfate (A.R.) initiator was added to 25 ml of water, and heated to  $70 \text{ }^\circ\text{C}$  before being added to the styrene mixture. The temperature was maintained at  $70 \pm 2 \text{ }^\circ\text{C}$  and the solution stirred at 300 rpm for 24 h. The resulting suspension was demulsified with 3.0 g  $\text{CaCl}_2$ , and then the suspension was filtered. Ethanol was used to wash away any un-reacted styrene. Finally, the PS nano-spheres were dried at  $60 \text{ }^\circ\text{C}$ .

### Preparation of $\text{LiFePO}_4/\text{C}$ cathode materials

$\text{LiFePO}_4/\text{C}$  powders were prepared by a solid state reaction method using  $\text{CH}_3\text{COOLi}$  (A.R.),  $\text{FeC}_2\text{O}_4 \cdot 2\text{H}_2\text{O}$  (A.R.), and  $\text{NH}_4\text{H}_2\text{PO}_4$  (A.R.; molar ratio of  $\text{Li}:\text{Fe}:\text{P}=1:1:1$ ) as starting materials, respectively, mixed with 7 wt.% four different carbon sources, such as PS nano-spheres, bamboo fiber, starch, and glucose. Then the precursors were ground in a planetary ball mill with a rotation speed of 280 rpm for 12 h in ethanol. After the mechanochemical processing, activated powders were heat-treated in a  $\text{N}_2/\text{H}_2$  (95%/5% in volume) atmosphere at  $400 \text{ }^\circ\text{C}$  for 4 h, then  $800 \text{ }^\circ\text{C}$  for 10 h. The four  $\text{LiFePO}_4/\text{C}$  samples by different carbon sources were obtained after cooling to room temperature.

### Characterization and electrochemical tests

Crystalline phases were identified by X-ray powder diffraction (XRD, XD-2, Persee) with  $\text{Cu K}\alpha$  radiation ( $\lambda=1.5406 \text{ \AA}$ ), and powder morphologies were observed by scanning electron microscopy (SEM, JEOL JSM-5400). Carbon structure was analyzed using Raman spectroscopy (Jobin Yvon, T64000).

Composite cathode electrode was fabricated by mixing as-prepared  $\text{LiFePO}_4/\text{C}$  powders (80 wt.%), carbon black (electronic conductive additive, 10 wt.%), and polyvinylidene fluoride (binder, 10 wt.%) in *N*-methylpyrrolidinone (NMP). This slurry was coated on aluminum foil and dried at  $100 \text{ }^\circ\text{C}$  overnight under vacuum. Electrochemical performance was tested by assembling CR2025 coin cells in a glove box filled with ultra pure argon, using lithium metal as the anode,  $1 \text{ M LiPF}_6$  dissolved in ethylene carbonate/dimethyl carbonate/ethylmethyl carbonate (EC:DMC:EMC; 1:1:1, v/v) as electrolyte and microporous polypropylene film (Celgard

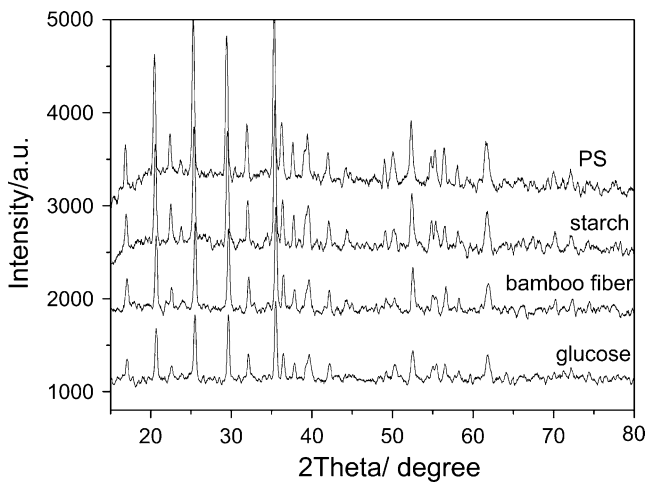


**Fig. 1** X-ray diffraction spectra of  $\text{LiFePO}_4/\text{C}$  composites prepared using various carbon sources

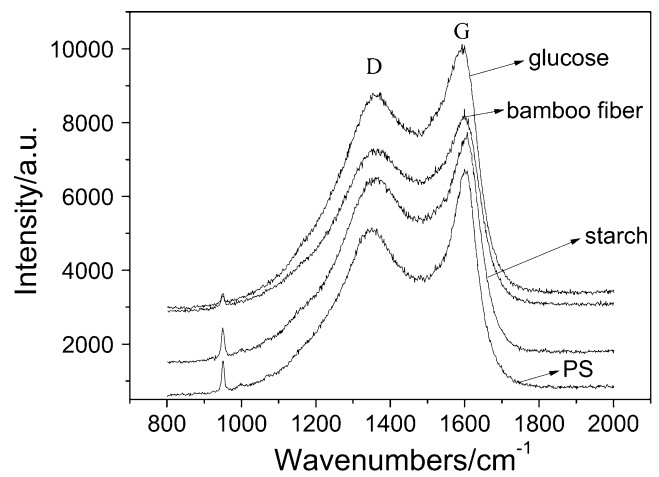
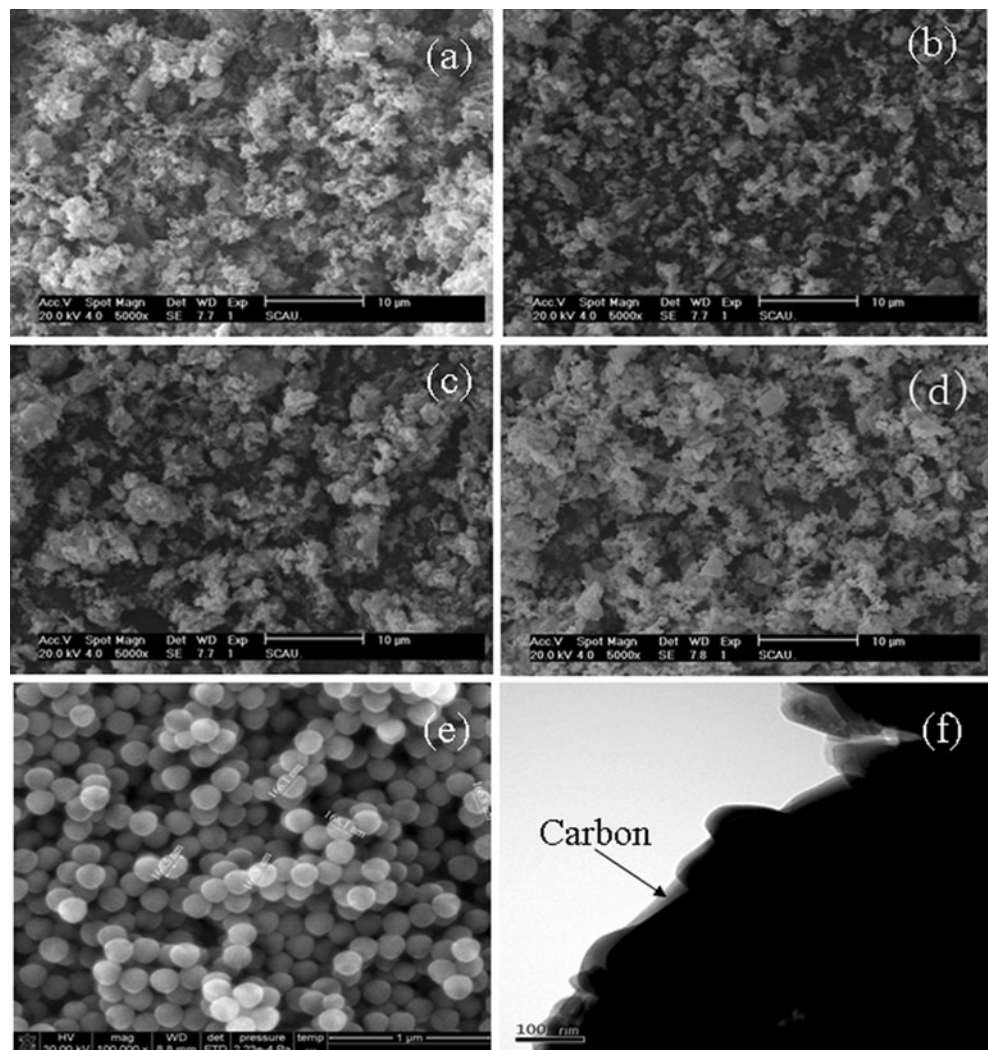


**Fig. 3** Raman spectra of  $\text{LiFePO}_4/\text{C}$  materials prepared using various carbon sources

2400) as a separator. Galvanostatic charge/discharge tests were performed at room temperature on a LAND CT-

2001A cell program control test system at various rates with cutoff voltages of 2.5 and 4.1 V vs.  $\text{Li}/\text{Li}^+$ . Electrochemical impedance spectroscopic (EIS) measure-

**Fig. 2** SEM images of  $\text{LiFePO}_4/\text{C}$  composites synthesized using various carbon sources: **a** PS nano-spheres, **b** starch, **c** bamboo fiber, **d** glucose. An SEM image of PS nano-spheres is shown in **(e)** and TEM image of  $\text{LiFePO}_4/\text{C}$  composite synthesized using PS in **(f)**



ments were carried out on an IM6e electrochemical workstation over the frequency range between 1 MHz and 10 mHz, applying a 5 mV alternating current signal.

## Result and discussion

### XRD analysis of LiFePO<sub>4</sub>/C

XRD patterns for LiFePO<sub>4</sub>/C composites from different carbon sources are shown in Fig. 1. All the patterns can be indexed to a single-phase material having an orthorhombic olivine-type structure with space group of *Pnma*, which corresponds to the reference LiFePO<sub>4</sub> spectrum (JCPDS card NO. 83–2029). No crystalline graphite phase can be identified from the XRD pattern, indicating that the coated carbon matrices are amorphous. This was further confirmed by Raman spectroscopy, which showed the appearance of a disorder-induced phonon mode (D) peak and graphite band (G) peak in the Raman spectrum of the LiFePO<sub>4</sub>/C composites. The results reveal that the synthesized product is composed of LiFePO<sub>4</sub> nanocrystals and amorphous carbon.

### SEM analysis of LiFePO<sub>4</sub>/C

The particle size and morphology of the composites were characterized by SEM. Figure 2 shows SEM images of the LiFePO<sub>4</sub>/C samples obtained from different carbon sources together with the SEM image of PS nano-spheres. As shown in Fig. 2e, the PS nano-spheres formed an almost opal structure with a narrow distribution of particle size and average diameter of 166 nm. The LiFePO<sub>4</sub>/C composites appear to have a submicrometer or micrometer grain size with irregular morphology (Fig. 2a–d). This suggests that carbon coating plays an important role in controlling the growth of the composite particles. A decrease in particle size results in a shortening of the diffusion path of Li<sup>+</sup> and improved electrochemical performance of LiFePO<sub>4</sub>/C compared to pure LiFePO<sub>4</sub> [25]. The transmission electron microscope (TEM) micrograph of the LiFePO<sub>4</sub>/C composite, obtained by the pyrolysis of PS nano-spheres, is shown in Fig. 2f. The relatively dark region of the figure represents LiFePO<sub>4</sub> surrounded by a carbon matrix, shown by the light gray layer, approximately 20–50 nm thick. From the TEM

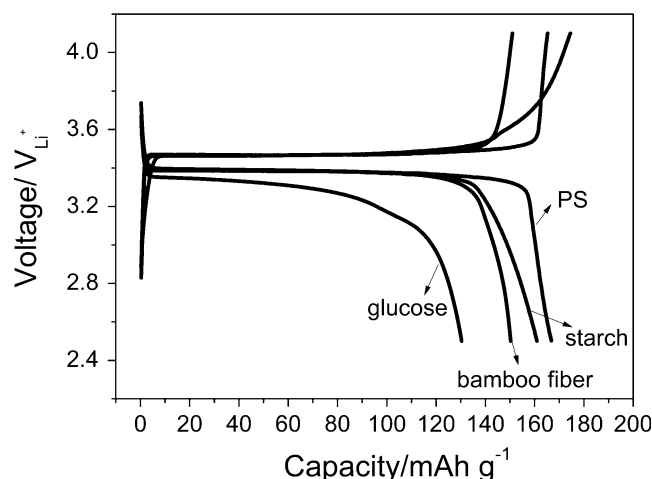


**Fig. 4** Initial charge–discharge curves for Li/LiFePO<sub>4</sub>/C cells at 0.1 C rate and cutoff voltages of 2.5 and 4.1 V vs. Li/Li<sup>+</sup>

images, it can be clearly seen that the entire carbon distribution surrounds the fine LiFePO<sub>4</sub> crystal grains. This carbon coating leads to electronic inter-grain connection, but does not block the direct contact between active particles and encapsulated electrolyte.

### Raman spectra analysis of LiFePO<sub>4</sub>/C composites

Raman spectroscopy is a particularly useful technique for characterizing the structure of the carbon-coating layer on the particles' surface. Figure 3 and Table 1 display the Raman spectra of the composites in the range of 800–1,800 cm<sup>-1</sup>. As shown in Fig. 3, all the Raman spectra consisted of a relatively small band at 950 cm<sup>-1</sup>, corresponding to the symmetric PO<sub>4</sub> stretching vibration of the LiFePO<sub>4</sub> olivine compound, and two intense broad bands at 1,350 and 1,605 cm<sup>-1</sup> that can be assigned to the D (disordered) and G (graphene) bands of the deposited carbon, respectively [26]. The D and G bands were numerically separated into four signals with a pseudo-Voigt profile function, located at 1,194, 1,347, 1,510, and 1,585 cm<sup>-1</sup>. The bands at 1,347 and 1,585 cm<sup>-1</sup> were ascribed to be *sp*<sup>2</sup> graphite-like structure, while the remaining bands were attributed to *sp*<sup>3</sup>-type carbon. The *I*<sub>D</sub>/*I*<sub>G</sub> ratio approximately correlates to the amount of graphene clusters in the disordered carbon, with smaller ratios being associated with higher electronic conductivity.

**Table 1** Parameters obtained from electrochemical impedance spectra and *I*<sub>D</sub>/*I*<sub>G</sub>, *sp*<sup>3</sup>/*sp*<sup>2</sup> ratios from Raman spectra for LiFePO<sub>4</sub>/C samples prepared using various carbon sources

Carbon source	<i>R</i> <sub>c</sub> /Ω	<i>R</i> <sub>ct</sub> /Ω	<i>i</i> <sub>0</sub> /mA·cm <sup>-2</sup>	<i>I</i> <sub>D</sub> / <i>I</i> <sub>G</sub> ratio	<i>sp</i> <sup>3</sup> / <i>sp</i> <sup>2</sup> ratio
PS	9.9	216.0	0.119	0.769	0.20
Starch	9.1	220.3	0.116	0.822	0.22
Bamboo fiber	7.4	293.5	0.087	0.856	0.24
Glucose	21.1	631.4	0.041	0.865	0.32

It is also possible to determine  $sp^3/sp^2$  ratios, with smaller ratios indicating a more graphitic structure, which has been associated with higher conductivity and enhanced electrochemical performance of  $LiFePO_4/C$  [27].

As shown in Table 1, the  $sp^3/sp^2$  ratio was estimated to be 0.20–0.35 for all carbon sources, indicating that the fraction of graphite-like carbon was 65–80% and the conducting path was mainly due to graphite-like carbon. It is interesting to note that the  $LiFePO_4/C$  sample prepared from PS nano-spheres had the lowest  $I_D/I_G$  and  $sp^3/sp^2$  ratios. In general, higher capacities and rate capability are associated with low values of  $I_D/I_G$  and  $sp^3/sp^2$ , which indicate a high degree of graphitization. Increasing the degree of graphitization can improve the electronic conductivity of residual carbon and thus provide better electronic contact between submicrometer particles with large agglomerates, resulting in improved electrode performance. The results described here are in agreement with the conclusions of Hadjean and Ramos [28] and Doeff et al. [29]. PS contains a large number of functionalized aromatic groups, which can lead to formation of more highly graphite-like carbons during pyrolysis, yielding composites with better electrochemical performance. This was supported by the electrochemical tests described below.

Electrochemical properties of  $LiFePO_4/C$

Figure 4 shows the initial charge and discharge profiles of  $Li/LiFePO_4/C$  cells at 0.1 C rate and in the voltage of 2.5–4.1 V. As shown in Fig. 4, there are two main parts contributing to the total discharge capacity. One is the plateau capacity at a voltage of about 3.4 V vs.  $Li^+/Li$ ; the other is the slop capacity between 3.4 and 2.5 V. This type of discharge profile has been observed previously in many systems with  $LiFePO_4/C$  composites [30, 31]. The broad

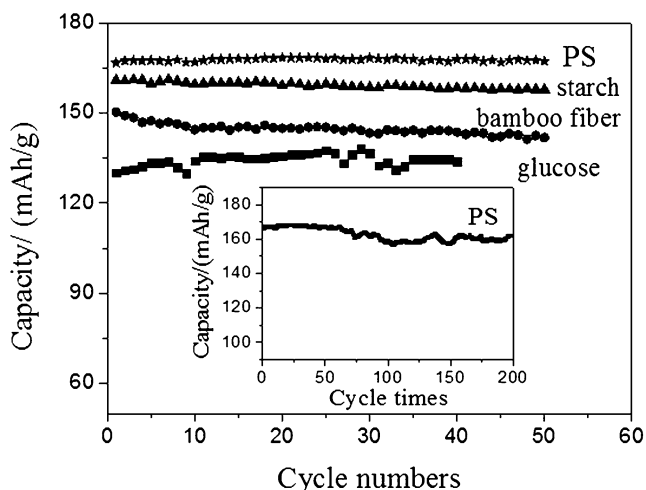


Fig. 5 Discharge capacities vs. cycle number for  $Li/LiFePO_4/C$  cells at a rate of 0.1 C and cycled between 2.5 and 4.1 V (vs.  $Li/Li^+$ )

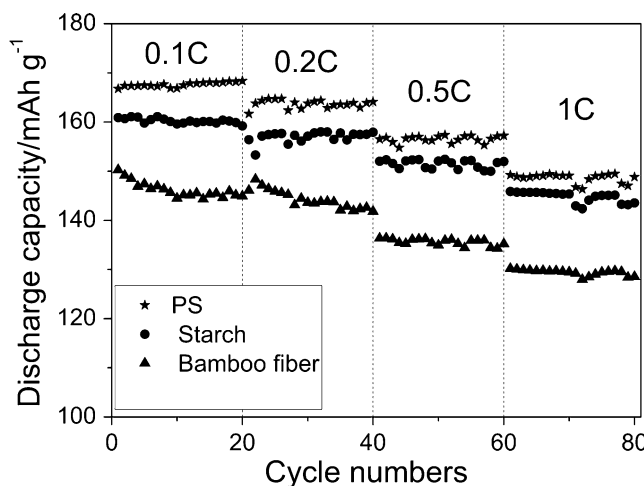


Fig. 6 Cycling performance, shown by discharge capacity over 20 cycles, of  $Li/LiFePO_4/C$  cells, at various rates using cutoff voltages of 2.5 and 4.1 V

plateaus in the charge–discharge curves at approximately 3.4 V (vs.  $Li/Li^+$ ) suggest that the extraction and insertion reactions of  $Li^+$  proceeds by the motion of a two-phase interface between  $FePO_4$  and  $LiFePO_4$  [32]. The voltage difference between the charge and discharge plateaus ( $\Delta V$ ) in Fig. 4 is related to the polarization of the cell system, with a smaller  $\Delta V$  indicating a lower polarization. As shown in Fig. 4, the  $LiFePO_4/C$  sample synthesized using PS nano-spheres delivers the largest discharge capacity of 167  $mAh\ g^{-1}$  at 0.1 C rate, corresponding to 98% of the theoretical capacity and also has the smallest  $\Delta V$  of 0.12 V. The small voltage difference between the charge–discharge plateaus indicates fast kinetics, due to the carbon forming a thin and uniform conductive film over the whole particle

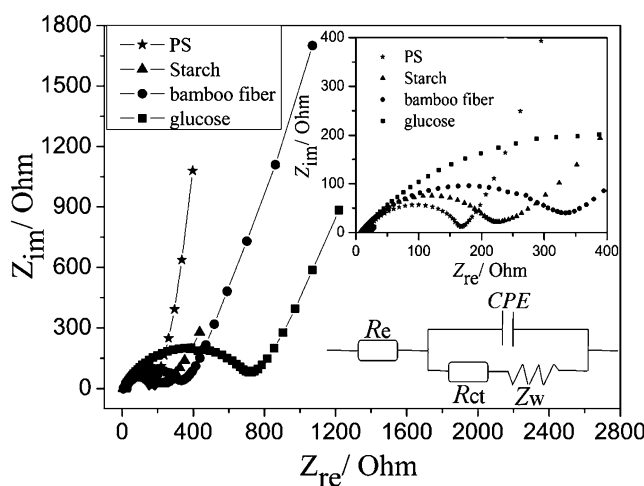


Fig. 7 EIS of  $Li/LiFePO_4/C$  cells prepared with various carbon sources, together with the equivalent circuit, where  $R_e$  is the electrolyte resistance,  $R_{ct}$  is the charge transfer resistance, CPE is the constant phase element, and  $Z_w$  the Warburg impedance

surface, improving the conductivity and contact between the electrolyte and the active phase [33].

The cycling performance at a discharge rate of 0.1 C, of Li/LiFePO<sub>4</sub>/C batteries prepared using different carbon sources, is shown in Fig. 5. All the cells displayed good capacity retention after 50 cycles. However, the cell discharge capacity depended on the carbon source. The sample synthesized using PS nano-spheres showed the best cycling performance of all four samples, with an initial discharge capacity of 167 mAh g<sup>-1</sup> and no degradation in capacity after 50 cycles.

In addition, Fig. 6 compares the discharge capacity of three of the LiFePO<sub>4</sub>/C composites at different discharge rates for 20 cycles. All samples displayed a decrease in discharge capacity as the discharge rate was increased, indicating that there are still significant performance limitations to be overcome. However, the LiFePO<sub>4</sub>/C from PS nano-spheres achieved the highest discharge capacity at all the discharge rates tested. Even at a rate of 1.0 C, a relatively high capacity of 150 mAh g<sup>-1</sup> was obtained, and there was no apparent degradation of the sample after cycling 20 times. This promising electrochemical performance may be due to the effect of the structure of the carbon source additive on the properties of the residual surface carbon of the LiFePO<sub>4</sub>/C composite. PS, containing polyaromatic hydrocarbons, enhances electronic conductivity of the material as a result of pyrolysis to graphite-like carbon, resulting in fast reaction and diffusion kinetics.

To study in detail the effect of carbon source on the electrochemical properties of composite cells, electrochemical impedance spectroscopy (EIS) measurements were carried out on CR 2025 coin cells. Figure 7 shows Nyquist plots obtained for the Li/LiFePO<sub>4</sub>/C cells containing different carbon additives and the equivalent circuit of the electrode system. In the AC impedance spectra, the depressed semicircles in the high-frequency region are attributed to the charge transfer process, with the charge transfer resistance ( $R_{ct}$ ) being equal to the diameter of the depressed semicircles. The linear plots in the low-frequency region are ascribed to typical Warburg behavior, which is attributed to the diffusion of lithium ions in the cathode material [34, 35]. The parameters of the equivalent circuit obtained using computer simulations are shown in Table 1. These values show that  $R_{ct}$  is the dominant factor governing Li ion transport. In Table 1,  $i_0$  denotes the exchange current density which is calculated from the following equation [36].

$$R_{ct} = \frac{RT}{Fi_0}$$

where  $R=8.315 \text{ JK}^{-1} \text{ mol}^{-1}$ ,  $F=96,500$ , and  $T=298.5 \text{ K}$ .

As shown in Table 1, LiFePO<sub>4</sub>/C synthesized using PS nano-spheres had the lowest  $R_{ct}$  and therefore the highest  $i_0$ . The low  $R_{ct}$  and high  $i_0$  values of this electrode material imply an increased ability of Li<sup>+</sup> to deintercalate and intercalate and are advantageous in reducing kinetic limitations during the charge and discharge processes. These results suggest that carbon from PS nano-spheres enhances the electrochemical performance of LiFePO<sub>4</sub>/C. In addition, the high conductivity of LiFePO<sub>4</sub>/C prepared with PS nano-spheres supports the Raman results described earlier, which showed a greater proportion of graphite-type carbon in this composite.

## Conclusions

In this study, LiFePO<sub>4</sub>/C composites were successfully prepared using various carbon sources: PS nano-spheres, bamboo fiber, starch, and glucose. XRD results showed that all the samples had an orthorhombic olivine-type structure. PS nano-spheres were found to be a suitable carbon source for producing LiFePO<sub>4</sub>/C composites with fine particle size, and uniform coating of the carbon conductive layer. Furthermore, Raman spectra demonstrated that most of the residual carbon produced by the pyrolysis of PS was graphite-like. Among the materials studied, LiFePO<sub>4</sub>/C synthesized with PS nano-spheres exhibited the best electrochemical performance, with the highest discharge capacity of 167 mAh g<sup>-1</sup> at 0.1 C rate and also the best rate capability. This sample also showed a lower charge transfer resistance and a higher exchange current density, as indicated by EIS.

The enhanced electrochemical performance of this composite could be attributed to the effect of the structure of the PS nano-spheres on the properties of the residual surface carbon. PS is a polycyclic compound containing many functionalized aromatic groups, which results in a greater proportion of graphite-like carbon being formed during polymer pyrolysis. Thus, composites prepared using PS nano-spheres exhibit fast reaction and diffusion kinetics with high discharge capacities and rate capability. These results demonstrate that the choice of carbon precursor is an important factor in optimizing the performance of LiFePO<sub>4</sub>/C composites.

**Acknowledgement** This research was supported financially by the Guangdong Natural Science Foundation (grant no. 9151064201000039), the Guangdong Science and Technology Planning Project (nos. 2009B010900025 and 2010B080701072), the National Natural Science Foundation of China (nos. 20963002 and 51003034), the Key Academic Program of the 3rd phase “211 Project” (no. 2009B010100001), the President of South China Agricultural University (no. K09140), and the Key Laboratory of Renewable Energy and Gas Hydrate Program of the Chinese Academy of Sciences (no. 2010002).

## References

1. Tarascon JM, Armand M (2001) *Nature* 414:359–367
2. Armand M, Tarascon JM (2008) *Nature* 451:652–657
3. Padhi AK, Nanjundaswamy KS, Goodenough JB (1997) *J Electrochem Soc* 144:1188–1194
4. Amin R, Balaya P, Maier (2006) *Electrochem Solid-State Lett* 10: A13–A16
5. Croce F, Epifanio AD, Hassoun J, Deptula A, Olczac T, Scrosati B (2002) *Electrochem Solid State Lett* 5:A47–A50
6. Park KS, Son JT, Chung HT, Kim SJ, Lee CH, Kang KT, Kim HG (2004) *Solid State Commun* 129:311–314
7. Chung SY, Bloking JT, Chiang YM (2002) *Nat Mater* 1:123–128
8. Wang D, Li H, Shi S, Huang X, Chen L (2005) *Electrochim Acta* 50:2955–2958
9. Cui G, Hu YS, Zhi L, Wu D, Lieberwirth I, Maier J, Mullen K (2007) *Small* 3:2066–2069
10. Cui G, Hu YS, Zhi L, Kaskhedikar N, Peter AA, Mullen K, Maier J (2008) *Adv Mater* 20:3079–3083
11. Wang YG, Wang YR, Hosono E, Wang KX, Zhou HS (2008) *Angew Chem Int Ed* 47:7461–7465
12. Huang YH, Park KS, Goodenough JB (2006) *J Electrochem Soc* 153:A2282–A2286
13. Park KS, Schougaard SB, Goodenough JB (2007) *Adv Mater* 19:848–851
14. Gibot P, Montse CC, Lydia L, Stephane L, Philippe C, Stephane H, Jean-Marie T, Christian M (2008) *Nat Mater* 7:741–747
15. Bilecka I, Hintennach A, Djerdj I, Novák P, Niederger M (2009) *J Mater Chem* 19:5125–5128
16. Doeff MM, Wilcox JD, Yu R, Aumentado A, Marcinek M, Kostecki R (2008) *J Solid State Electrochem* 12:995–1001
17. Cho YD, Feyta GT, Kao HM (2009) *J Power Sources* 189:256–262
18. Konarova M, Taniguchi I (2010) *J Power Sources* 195:3661–3667
19. Chen Z, Dahn JR (2002) *J Electrochem Soc* 149:A1184–1189
20. Nakano H, Dokko K, Koizumi S, Tannai H, Kanamura K (2008) *J Electrochem Soc* 155:A909–A914
21. Cushing BL, Goodenough JB (2002) *Solid State Sci* 4:1487–1493
22. Choi D, Kumta P (2007) *J Power Sources* 163:1064–1069
23. Ong CW, Lin YK, Chen JS (2007) *J Electrochem Soc* 154:A527–A533
24. Nien YH, Carey JR, Chen JS (2009) *J Power Sources* 193:822–827
25. Goktepe G, Halil S, Fatma K, Patat S (2010) *Ionics* 16:203–208
26. Bhuvanawari MS, Bramnik NN, Ensling D, Ehrenberg H, Jaegermann W (2008) *J Power Sources* 180:553–560
27. Nakamura T, Miwa Y, Tabuchi M, Yamada Y (2006) *J Electrochem Soc* 153:A1108–A1114
28. Hadjean RB, Ramos JPP (2010) *Chem Rev* 110:1278–1219
29. Doeff MM, Hu Y, McLarnon F, Kosteckib R (2003) *Electrochem Solid-State Lett* 6:A207–A209
30. Liu J, Jiang R, Wang X, Huang T, Yu A (2009) *J Power Sources* 194:536–540
31. Kim DH, Kim JS, Kang JW, Kim EJ, Ahn HY, Kim J (2007) *J Nanosci Nanotechnol* 7:3949–3953
32. Delmas C, Maccario M, Croguennec L, Le CF, Weill F (2008) *Nat Mater* 7:665–671
33. Kim JK, Cheruvally G, Ahn JH (2008) *J Solid State Electrochem* 12:799–805
34. Li X, Wang W, Shi C, Wang H, Xing Y (2009) *J Solid State Electrochem* 13:921–926
35. Jin B, Jin EM, Park KH, Gu HB (2008) *Electrochem Commun* 10:1537–1540
36. Gao F, Tang Z (2008) *Electrochim Acta* 53:5071–5075